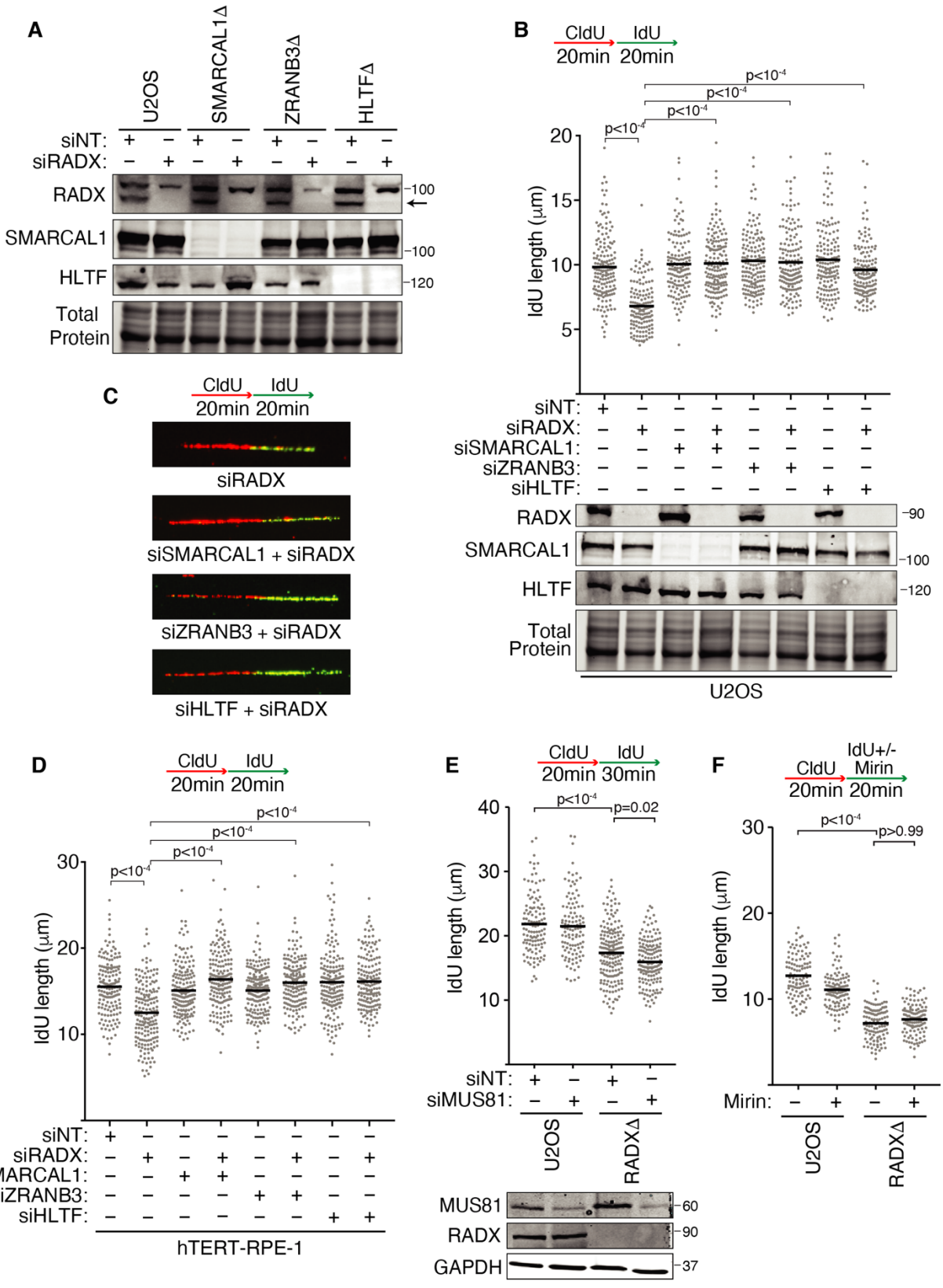
A
U2OS
SMARCAL1Δ
ZRANB3Δ
HLTFΔ
siNT:
siRADX:
RADX
SMARCAL1
HLTF
Total Protein
B
CldU 20min
IdU 20min
IdU length (μm)
siNT:
siRADX:
siSMARCAL1:
siZRANB3:
siHLTF:
RADX
SMARCAL1
HLTF
Total Protein
U2OS
C
CldU 20min
IdU 20min
siRADX
siSMARCAL1 + siRADX
siZRANB3 + siRADX
siHLTF + siRADX
D
CldU 20min
IdU 20min
IdU length (μm)
siNT:
siRADX:
siSMARCAL1:
siZRANB3:
siHLTF:
hTERT-RPE-1
E
CldU 20min
IdU 30min
p=0.02
IdU length (μm)
siNT:
siMUS81:
U2OS
RADXΔ
MUS81
RADX
GAPDH
F
CldU 20min
IdU+/- Mirin 20min
p>0.99
IdU length (μm)
Mirin:
U2OS
RADXΔ

Supplementary Figure 1. Aberrant fork reversal causes fork collapse in RADX-deficient cells (related to Figure 1). (A) Immunoblots of U2OS and SMARCAL1Δ, ZRANB3Δ, and HLTFΔ cell lysates after transfection of the indicated siRNAs (siNT = non-targeting). (B) Replication elongation rate was measured by DNA fiber spreading after transfection of U2OS cells with siRNAs. Immunoblots of cell lysates are shown. (C) Representative DNA combing images of replication tracts stained with antibodies to CldU and IdU. (D) Replication elongation rate was measured by DNA combing after transfection of hTERT-RPE-1 cells with siRNAs. (E and F) Replication elongation rate was measured by DNA combing (E) or fiber spreading (F) in wild-type or RADXΔ U2OS cells transfected with the indicated siRNA or treated with 100μM Mirin. All experiments were completed at least twice. A one-way ANOVA with Tukey's multiple comparison test was used to calculate p values for all fiber experiments.

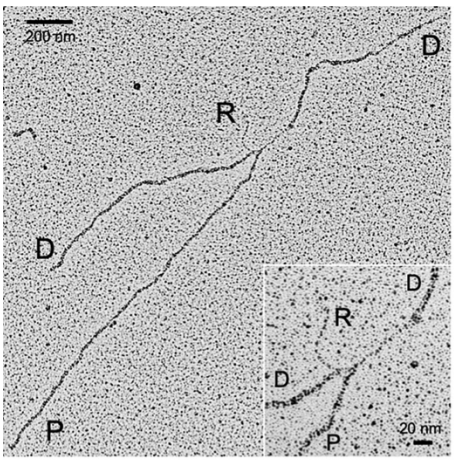
200 nm
D
R
D
P
R
D
D
P
20 nm

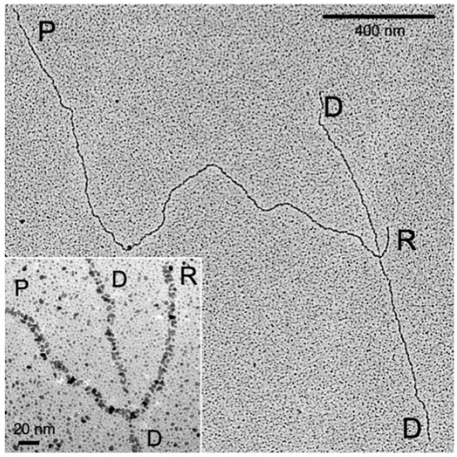
P
400 nm
D
R
P
D
R
20 nm
D
D

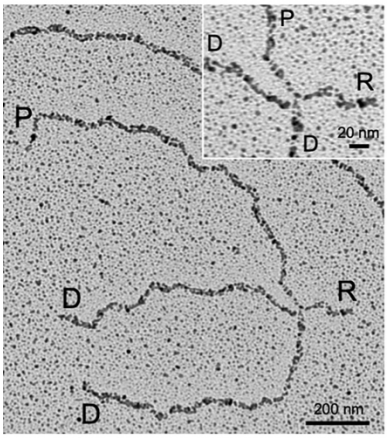
P
D
R
D
20 nm
P
D
R
D
R
D
200 nm

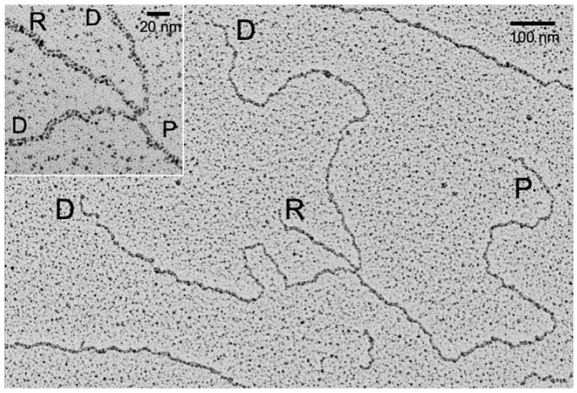
R
D
20 nm
D
P
100 nm
D
D
R
P

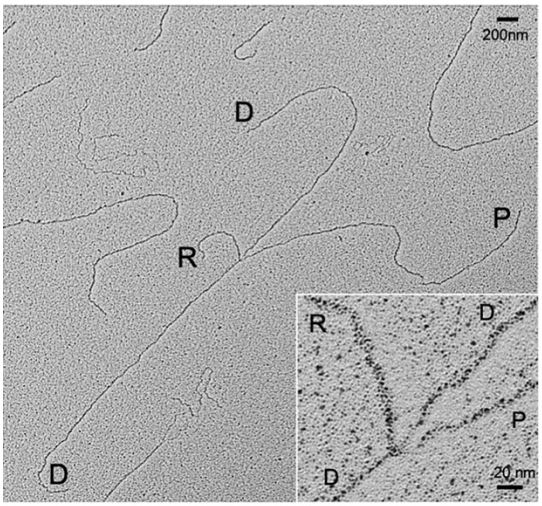
200nm
D
P
R
R
D
P
D
D
20 nm

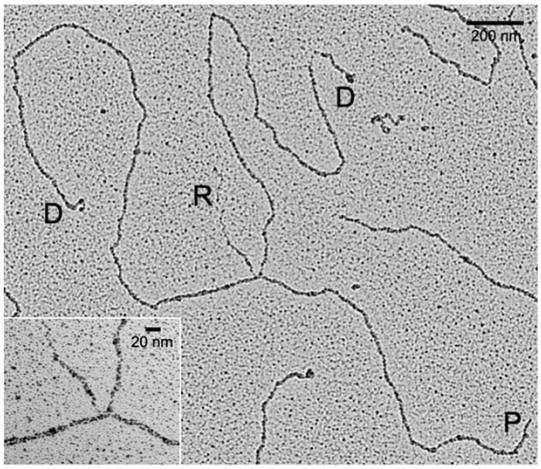
200 nm
D
D
R
20 nm
P

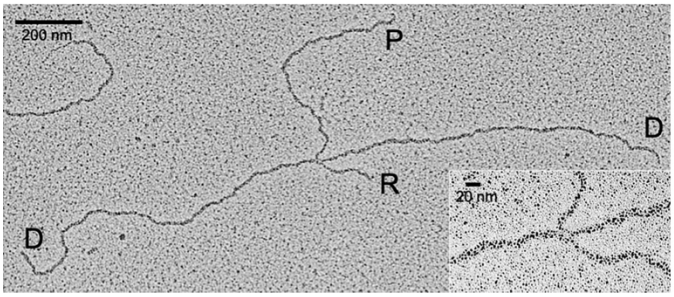
200 nm
P
D
R
20 nm
D

Supplementary Figure 2. Representative EM images. (related to Figure 1) Representative EM images are shown. Inset, magnified four-way junction at the reversed fork; P, parental strands; D, daughter strands; R, reversed strands

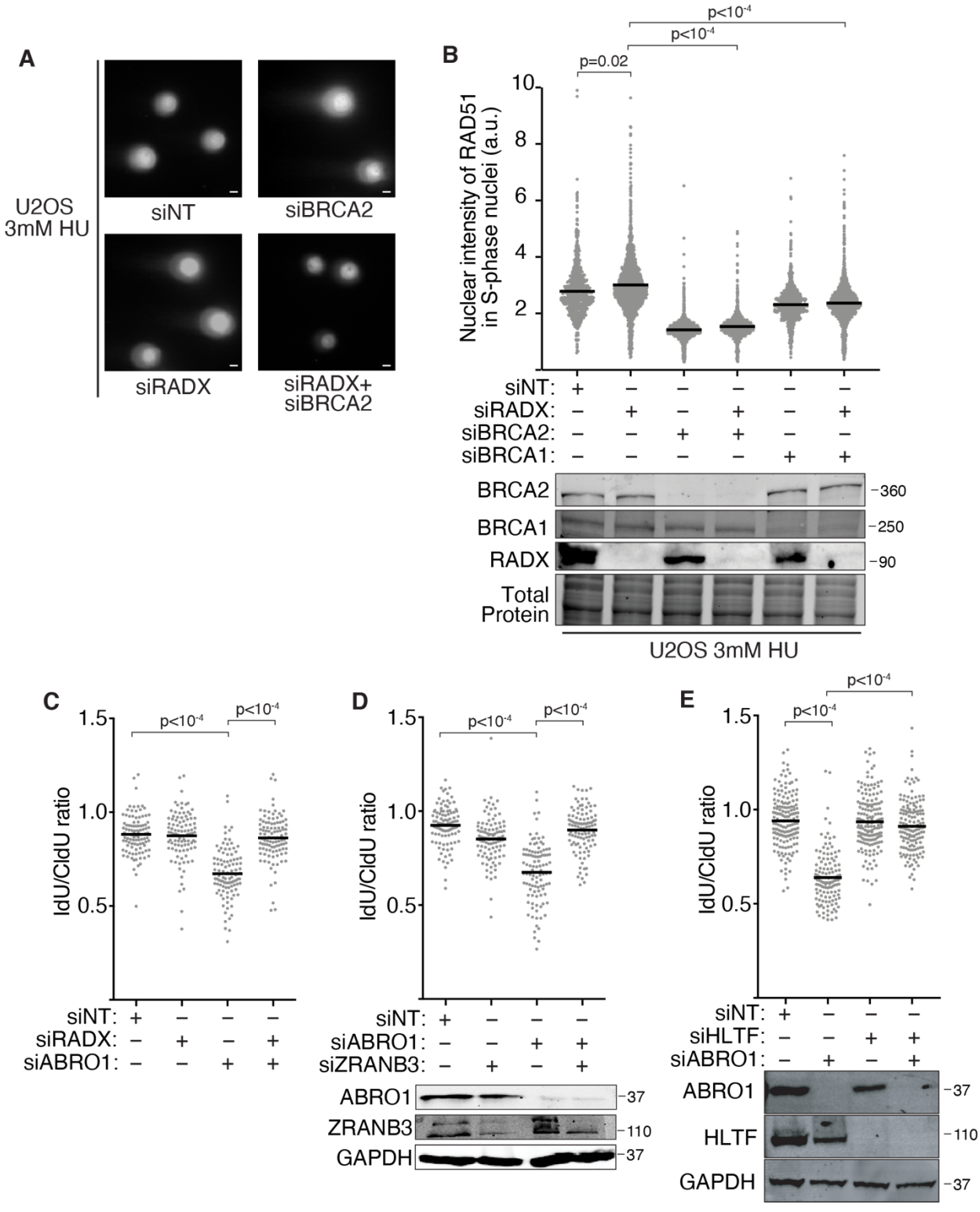

Supplementary Figure 3. RADX inactivation rescues fork protection without restoring RAD51 localization to stalled forks in BRCA1- or BRCA2-deficient cells. (related to Figure

2) (A) Representative images of neutral comet assay in U2OS cells transfected with the indicated siRNAs and treated with 3mM HU for 5h. Scale bar-10μm (B) RAD51 localization was assessed by immunofluorescence imaging in cells transfected with the indicated siRNAs and treated with 3mM HU for 5h. Soluble RAD51 was removed by detergent pre-extraction. An immunoblot shows protein levels. A Kruskal-Wallis test was used to calculate p values. (C-E) Fork protection assays were performed in U2OS cells transfected with the indicated siRNAs. A one-way ANOVA with Tukey's multiple comparison test was used to calculate p values for all fiber experiments.

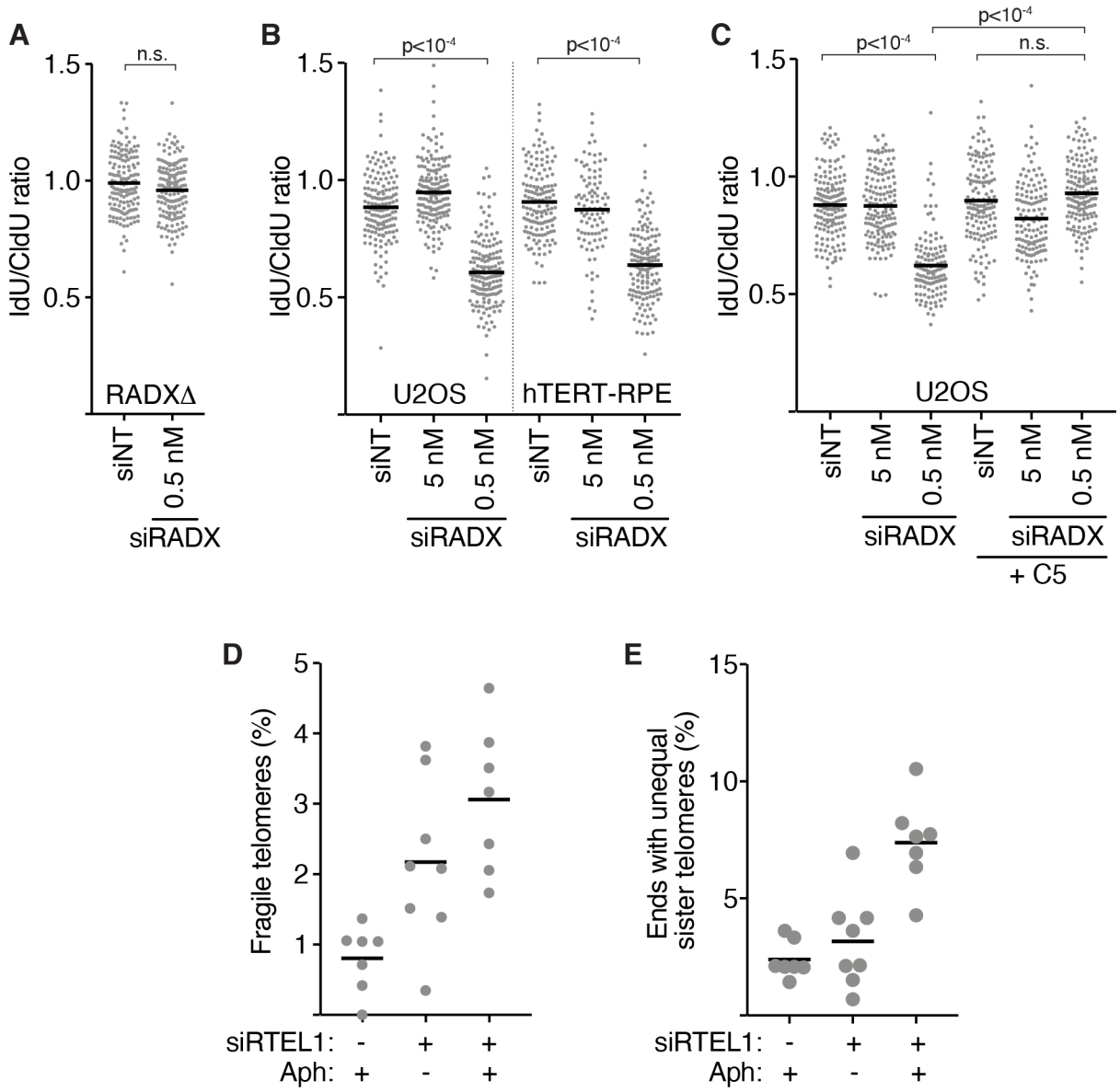

Supplementary Figure 4. Partial silencing of RADX causes nascent strand degradation while addition of aphidicolin increases telomere catastrophe in RTEL1-deficient cells. (related to Figures 3 and 4) (A-C) Fork protection assays were performed after transfection with 0.5 or 5nM of RADX siRNA #21 or 5nM non-targeting (NT) siRNA. Transfections with 0.5nM of RADX siRNA were supplemented with NT siRNA to reach a total of 5nM. Cells were treated with 20μM of the C5 DNA2 inhibitor where indicated. A one-way ANOVA with Tukey's multiple comparison test was used to calculate all p values. (D) Quantification of fragile telomeres and (E)

telomere heterogeneity in cells transfected with the indicated siRNAs and treated with or without 0.2μM aphidicolin for 40h.

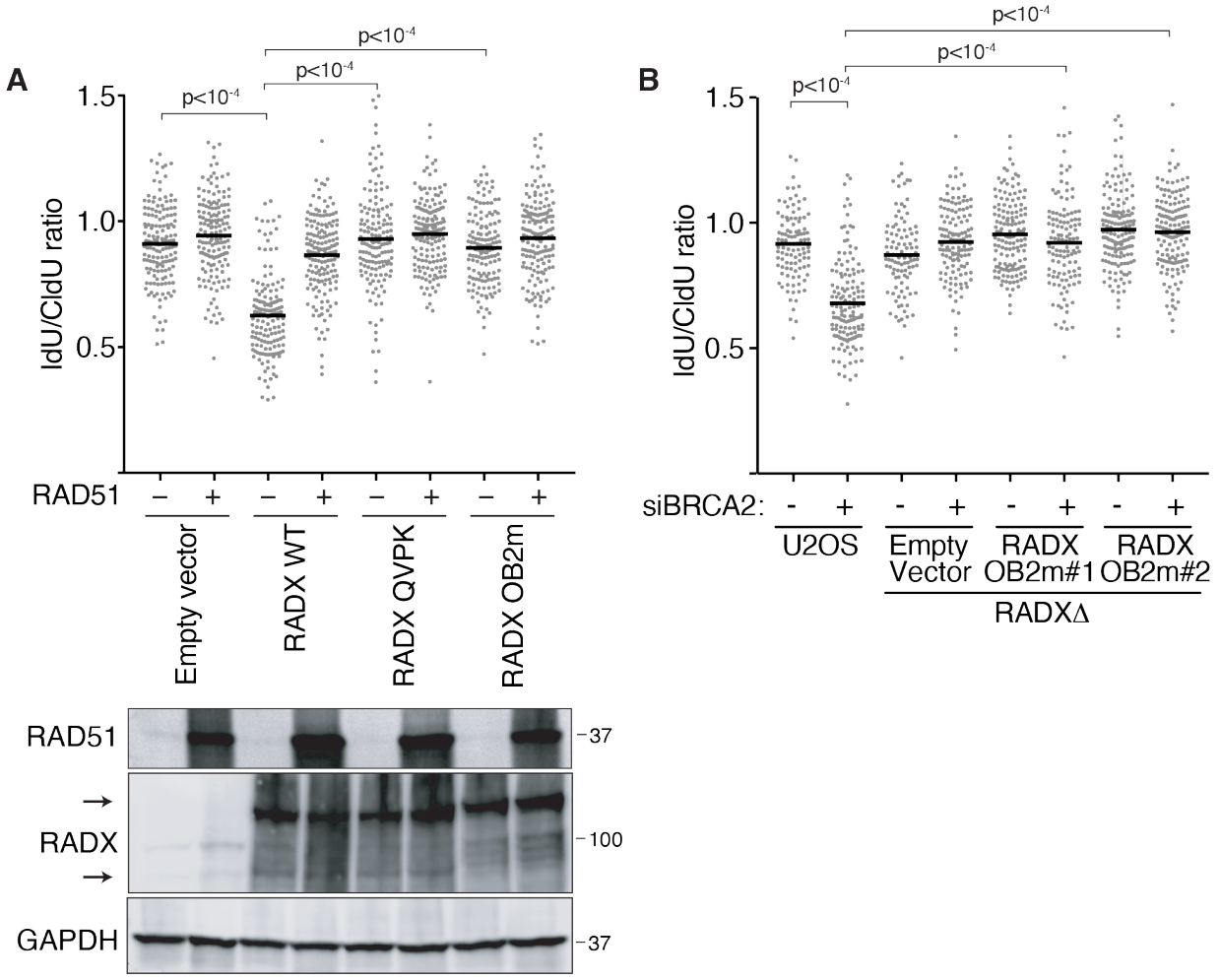

Supplementary Figure 5. Interaction of RADX with single strand DNA and RAD51 is required for nascent strand degradation in cells treated with HU. (related to Figure 5) (A) Fork protection assays were performed in HU-treated cells transiently overexpressing either wild-type RADX, QVPK RADX, or OB2m RADX and wild-type RAD51 as indicated. (B) Wild-type U2OS, RADXΔ U2OS cells (empty vector), or two clones of RADXΔ cells complemented with RADX OB2m (Dungrawala et al., 2017), were transfected with non-targeting or BRCA2 siRNA as indicated. Fork protection assays were completed. Arrows in the immunoblot indicate the endogenous and GFP-FLAG-tagged RADX proteins. A one-way ANOVA with Tukey's multiple comparison test was used to calculate all p values. All experiments were completed at least two times.

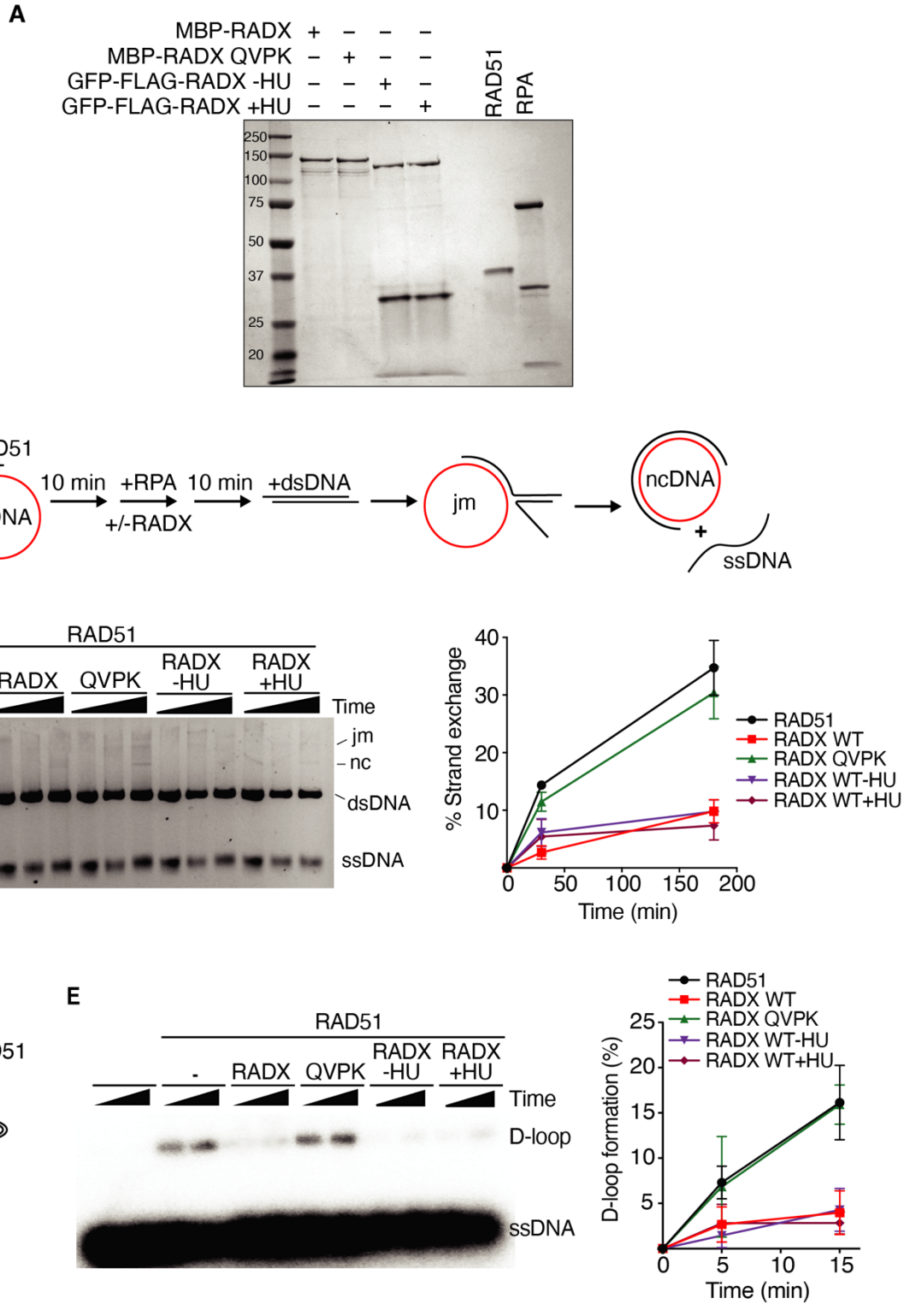
A
MBP-RADX + – – –
MBP-RADX QVPK – + – –
GFP-FLAG-RADX -HU – – + –
GFP-FLAG-RADX +HU – – – +
RAD51
RPA
250
150
100
75
50
37
25
20
B
RAD51
+
ssDNA
10 min
+RPA
10 min
+dsDNA
+/-RADX
jm
ncDNA
+
ssDNA
C
RAD51
-RPA
-
RADX
QVPK
RADX -HU
RADX +HU
Time
jm
nc
dsDNA
ssDNA
% Strand exchange
40
30
20
10
0
50
100
150
200
Time (min)
RAD51
RADX WT
RADX QVPK
RADX WT-HU
RADX WT+HU
D
ssDNA
RAD51
+
+/-RADX
D-loop
E
RAD51
-
RADX
QVPK
RADX -HU
RADX +HU
Time
D-loop
ssDNA
D-loop formation (%)
25
20
15
10
5
0
5
10
15
Time (min)
RAD51
RADX WT
RADX QVPK
RADX WT-HU
RADX WT+HU

Supplementary Figure 6. RADX purified from unstressed and HU-treated cells inhibits strand exchange and D-loop formation. (related to Figure 5) (A) Coomassie stained SDS-PAGE gel showing purified proteins used in this study. Each lane contains ~200 nM of purified protein. Actual amounts used is specified in each experiment. MBP-RADX and MBP-RADX QVPK were purified from insect cells while FLAG-GFP-RADX -HU and FLAG-GFP-RADX +HU were purified from 293T cells that were synchronized in S-phase and either harvested immediately or treated with 3mM HU for 5 hours before harvesting. (B) Schematic of strand exchange experiment (jm, joint molecules; nc, nicked circular dsDNA). (C) A representative gel and quantitation of n=3 strand exchange assays are shown. Error bars are SD. (D) Schematic of displacement loop assay. (E) Representative gel of the D-loop assay and quantitation of n=3 (mean+/-SD).

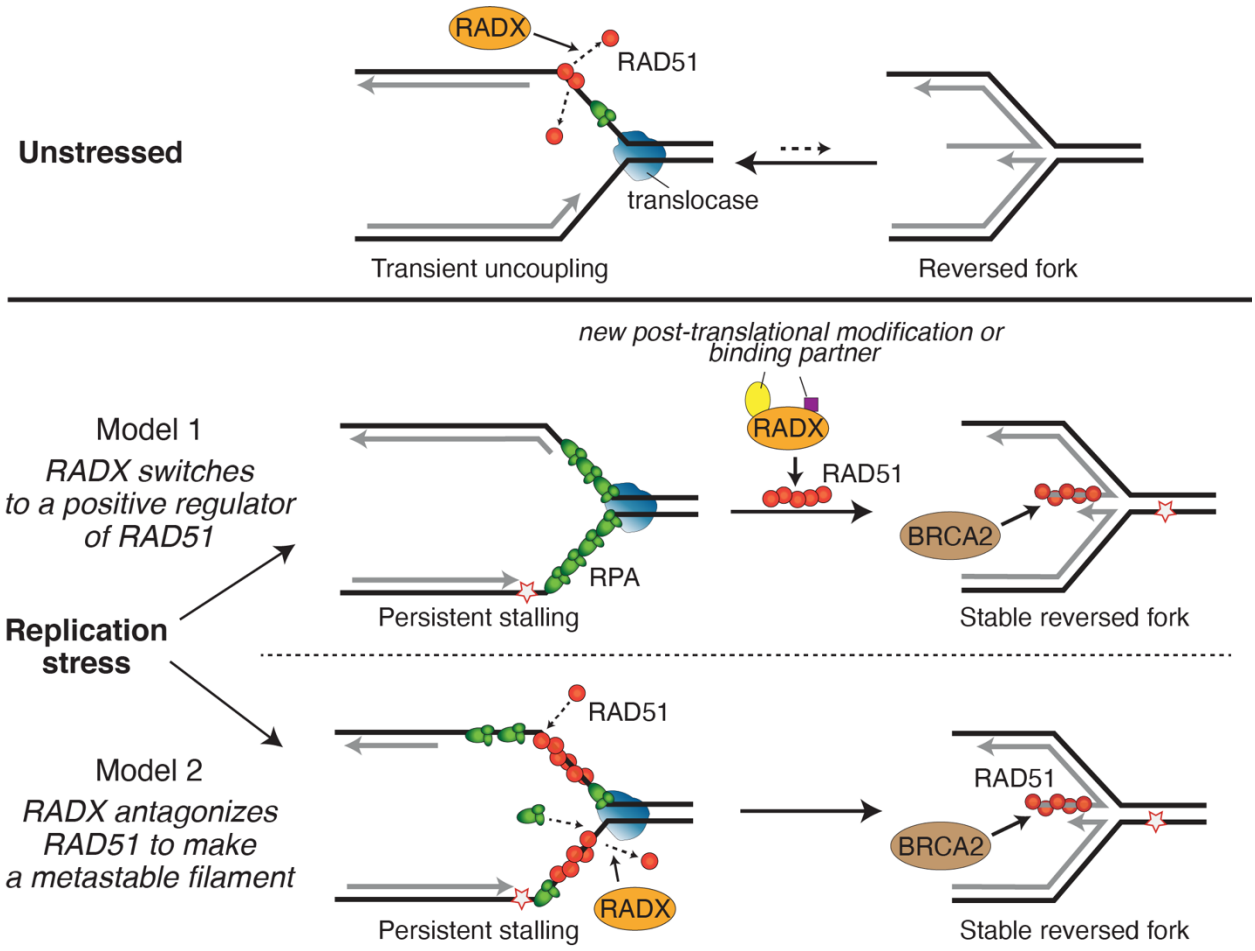

Figure S7. Models for RADX function in the absence and presence of added replication stress. (related to Figure 7) RADX directly binds to ssDNA and RAD51, increases RAD51 ATP hydrolysis rates, and destabilizes RAD51 filaments (Adolph et al., 2021). In unstressed cells, RADX may displace RAD51 bound to ssDNA that is exposed on the lagging strand or during transient uncoupling of leading and lagging strand polymerization. This activity prevents fork reversal. Upon addition of replication stress, more extensive ssDNA is generated, and RADX is required to promote fork reversal. In model 1, RADX may gain a post-translational modification or binding partner to switch from an antagonist to an activator of RAD51. Alternatively, in model 2, RADX may be required to displace RAD51 from ssDNA to promote the formation of a metastable RAD51 filament for fork reversal.